Assessment of future water availability under climate change, considering scenarios for population growth and ageing infrastructure

Erle Kristvik, Tone M. Muthanna and Knut Alfredsen

ABSTRACT

Climate change is likely to cause higher temperatures and alterations in precipitation patterns, with potential impacts on water resources. One important issue in this respect is inflow to drinking water reservoirs. Moreover, deteriorating infrastructures cause leakage in water distribution systems and urbanization augments water demand in cities. In this paper, a framework for assessing the combined impacts of multiple trends on water availability is proposed. The approach is focused on treating uncertainty in local climate projections in order to be of practical use to water suppliers and decision makers. An index for water availability (WAI) is introduced to quantify impacts of climate change, population growth, and ageing infrastructure, as well as the effects of implementing counteractive measures, and has been applied to the city of Bergen, Norway. Results of the study emphasize the importance of considering a range of climate scenarios due to the wide spread in global projections. For the specific case of Bergen, substantial alterations in the hydrological cycle were projected, leading to stronger seasonal variations and a more unpredictable water availability. By sensitivity analysis of the WAI, it was demonstrated how two adaptive measures, increased storage capacity and leakage reduction, can help counteract the impacts of climate change.

Key words | adaptation, climate change, leakages, statistical downscaling, water availability, water supply

Erle Kristvik (corresponding author)
Tone M. Muthanna
Knut Alfredsen
Department of Civil and Environmental
  Engineering,
NTNU,
Trondheim 7491,
Norway
E-mail: *erle.kristvik@ntnu.no*

INTRODUCTION

A safe and steady drinking water supply is one of the most important public goods there is. As awareness of climate change increases, there is rising concern for the future reliability of drinking water supplies. Climate change is likely to cause higher temperatures and alter precipitation patterns (IPCC 2013) and the understanding of the local impacts of this on the hydrological cycle is highly relevant for planning a provident water supply. At the same time, more and more people live in cities, yielding more strain on existing water supply systems as the water demand

increases in pace with population growth. In addition, many cities experience high levels of water losses due to ageing infrastructure and deteriorating pipes. Responsible water suppliers need to assess both the potential negative effects of climate change to supply and the trends towards increased water demand if they wish to secure reliable water supply services in the future.

There exist numerous studies of the impacts of climate change on the hydrological cycle, water resources, and availability, see for instance Barnett *et al.* (2008) or Schewe *et al.* (2014). The impacts are estimated by hydrological models that are driven by the input of meteorological variables such as temperature, precipitation, and evapotranspiration. Thus, the hydrological impacts of climate change may be

estimated by using projected values of the meteorological input variables required by the model. Global climate models (GCMs) are the primary source for projections of future climate, being comprehensive numerical models that simulate the past and future responses to external forces, such as greenhouse gases in the atmosphere (IPCC 2013). Representative concentration pathways (RCPs) are the state-of-the-art scenarios of future emissions in terms of the net radiative flux changes (W m^{-2}) in the year 2100 (Moss *et al.* 2010). The most recent group of scenarios consist of four scenarios: RCP2.6, RCP4.5, RCP6.0, and RCP8.5, where the number in each scenario name indicates the level at which the net radiative-flux change will stabilize by the end of the 21st century.

Over the last decades, GCMs have evolved and become more and more detailed. However, they are limited by coarse spatial and temporal resolutions and need further downscaling before they can be applied in local-scale studies (e.g. Fowler *et al.* 2007; Maraun *et al.* 2010). Several techniques for downscaling have been developed and they vary from dynamical to statistical approaches. Dynamical downscaling involves the nesting of a regional climate model within the boundaries of a GCM, such that sub-GCM grid scale features are simulated (Wilby *et al.* 2002). Statistical downscaling focuses on the statistical relationship between some large-scale variable and the local climate, defined by Benestad *et al.* (2008) as 'the process of making the link between the state of some variable representing a large space and the state of some variable representing a much smaller space'. Compared with the statistical approach, a strength of dynamical downscaling is that it is based on physics and resolving of atmospheric processes at the local level (Wilby *et al.* 2002). However, the application of dynamical downscaling requires significant computing resources compared with statistical models, which are also more flexible because they can be adapted to other regions other than the ones for which they are built. Some of the statistical downscaling techniques have resulted in practical tools, which contributes to making climate scenarios more available to impact assessors. Examples of such are the statistical downscaling software *SDSM* (Wilby *et al.* 2002) and the *R*-package '*esd*' by Benestad *et al.* (2015).

The availability of climate projections for impact studies are improving (CMIP5 2013), but there are still challenges related to handling the uncertainty of the projections. Ekström *et al.* (2015) categorized the uncertainty in climate projections into the uncertainty related to external forces (Type I), the uncertainty related to the climate system's response to these forces (Type II), and uncertainty due to natural variability (Type III). The paper argues that Type I uncertainty is handled using different emissions scenarios. Furthermore, using multi-model ensembles (ensembles of different GCMs) and perturbed physics ensembles (ensemble of one GCM with differing initial conditions and parameter schemes) should account for Type II and Type III uncertainty, respectively. Giorgi & Mearns (2003) proposed the 'Reliability Ensemble Averaging' method for assessing the reliability of simulated changes in multi-model GCM runs. The method involves quantifying the reliability of regional GCM simulations by combining two reliability criteria that accounts for: (1) the models' ability to reproduce historical and present day climate (the model performance criterion); and (2) the convergence of the models' simulated climate to the ensemble mean (the model convergence criterion). By following this framework it is possible to assess the probability of climate projections exceeding given thresholds and reduce predictive uncertainty in hydrological impacts studies (Giorgi & Mearns 2003).

GCM ensembles, downscaling, and reliability-weighted projections add valuable information that enables a better understanding of the future climate. However, the intrinsic uncertainty that accompanies the climate scenarios and projections makes it complicated to use them as a basis for decision making. Local water managers and stakeholders are still in need of easy-to-use tools that facilitate the assessment of water vulnerability (Sullivan 2011) and enable decision making and that are robust to the uncertainties of the future climate (Fowler *et al.* 2007). Thus, several studies have focused on the development of such tools, usually expressed as metrics or indexes that can quantify and measure the levels of impacts (see, for example, the robustness index defined by Whateley *et al.* (2014), or an overview of existing water vulnerability indices by Plummer *et al.* (2012)). Furthermore, Xia *et al.* (2012) defined water vulnerability as the ratio between the sensitivity of a water system to climate change and the adaptive capacity of the same system, and employed the framework to a case study in China. Their results led to the conclusion that water

management in China needs to shift from supply-oriented to demand-oriented management.

Recent studies of water resources availability under climate change in the city of Bergen, Norway, suggests a potential conflict between water supply and demand unless water losses in the distribution network are reduced (Kristvik & Riisnes 2015). Accordingly, water supply security could improve by making changes at the demand side of water management (i.e. reduce leakages). However, the study also highlights the need for practical tools that both reveal a supply system's vulnerability to external factors, such as climate change and population growth, and shows the system response and sensitivity to changes in conditions that decision makers can control, such as leakage rates (demand side) and levels of installed storage capacity (supply side).

This paper suggests a framework for assessing future water availability in cities with the aim of resolving some of the issues described in this section. These are, specifically: (1) high levels of uncertainty in local climate projections; and (2) lack of easy-to-use tools to facilitate water availability assessments. To address the first issue, a large ensemble of climate data is statistically downscaled and the site-specific projections are prepared. Furthermore, an index for water availability (WAI) is introduced. This index accounts for climate change as well as other straining factors that cities may experience, such as population growth and deteriorating infrastructure for water supply. Finally, a demonstration of the WAI is presented through scenario and sensitivity analyses where the effects of counteractive measures that reduce negative impacts on water availability are investigated.

MATERIALS AND METHODS

Study area

Bergen is the second largest city in Norway and located on the west coast of the country. The climate is wet and mild with an annual normal precipitation of 2250 mm and mean annual temperature of 7.6 °C (monthly normal values for 50540 Florida Weather Station, http://www.eklima.no/). Bergen is a particularly rainy city due to its exposure to westerly winds and the pronounced topography

characterizing the city. Statistically, the spring and summer months represent the driest period (see Figure 1 in Results and Discussion section). Usually, this does not conflict with water supply as snowmelt in this period makes up for lower precipitation amounts. However, the city has experienced substantial dry periods that have challenged water supply. The latest incident was in winter 2009–2010 when the climate was unusually dry and cold. At the turning point, water levels had dropped to half of their usual levels (Kristvik & Riisnes 2015).

The raw water serving the water supply system in the city is drawn from several reservoirs located close to the city centre and the water is treated at five major treatment plants: Svartediket, Jordalsvatnet, Espeland, Kismul, and Sædalen. Water from these plants is supplied to the inhabitants of Bergen through a distribution system comprising 900 km of pipe network. The network is complemented by transfer tunnels between treatment plants, securing a steady supply even if one plant is out of service (Bergen Municipality 2015).

Most (97%) of the total population of 278,000 inhabitants in Bergen are connected to the municipal water supply. In 2014 the estimated domestic consumption amounted to 45% of the produced drinking water, 21% was consumed by industry and 31% was ascribed to leakages in the distribution network (3% unspecified) (Bergen Municipality 2015; Statistics Norway 2016a). The municipality is continuously working on reducing the high level of leakages and the objective is to achieve a leakage level that equals 20% of produced water by 2024 (Bergen Municipality 2015). However, regional centres in Norway, such as Bergen, are expected to experience high population growth due to urbanization (Tønnessen & Leknes 2016). Thus, although the municipality is working on reducing water production by rehabilitating leaking pipes, the overall consumption is expected to increase as there are strong indications of continued population growth throughout the 21st century.

Projections of future climate

Output from GCMs is available through the Coupled Model Intercomparison Project phase 5 (CMIP5). The projections of temperature and large-scale precipitation for all available emissions scenarios (RCP2.6, RCP4.5, RCP6.0, and RCP8.5)
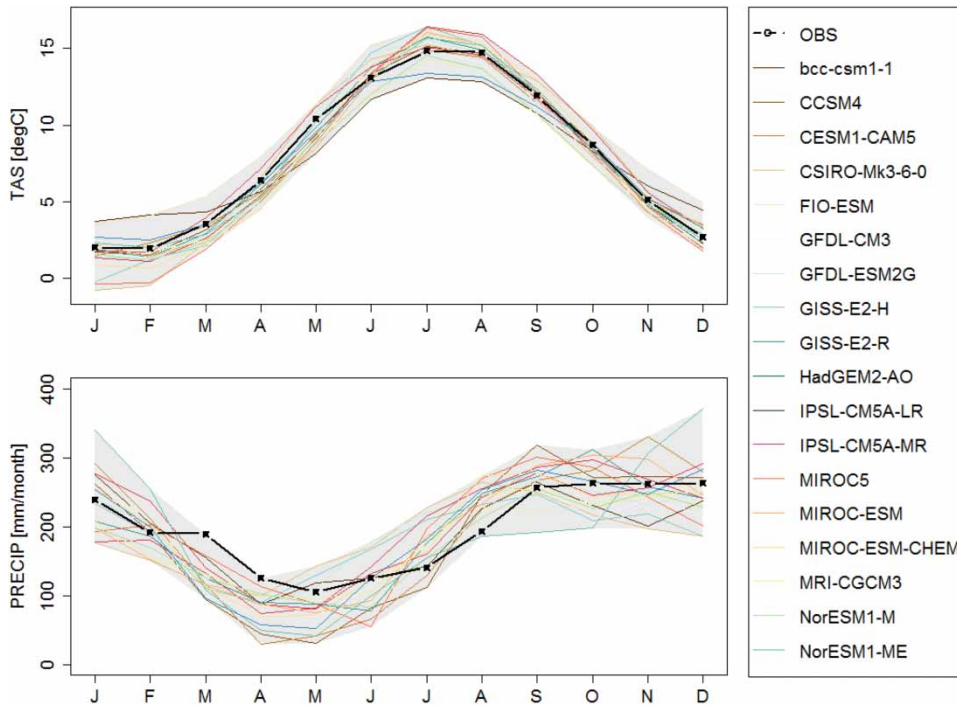
Figure 1 │ Historical climatology (1975–2005) from downscaled GCMs. The lines express the observed and simulated climatology, while the shaded areas represent the range of climatology simulated by the downscaled GCMs.

and from a selection of GCMs (Table 1) were statistically downscaled. The GCMs were selected based on a criterion that the results had to be comparable across emissions scenarios. Thus, only models that were run with all RCPs were selected. In addition, only GCM output from simulations with the same realization ID were selected. Based on this, the total number of common GCMs was 19. The downscaling was performed following the statistical approach as described by Benestad *et al.* (2008) and using tools provided by Benestad *et al.* (2015). The gridded datasets of observed temperature and large-scale precipitation from the NCAR/NCEP reanalysis (Kalnay *et al.* 1996) were combined with gridded projections of the same variables from GCMs to create common empirical orthogonal functions (EOFs). The common EOFs were used to fit a linear regression between the principal components of the EOFs and station data of observed temperature and precipitation from 50540 Florida Weather Station in Bergen. The regression model was calibrated with station data from the period 1975–2005 and gridded NCEP/NCAR reanalysis with a monthly time resolution. The obtained statistical relation was then employed to the GCM outputs to project monthly precipitation and monthly temperature at the Florida Weather Station for the period 2006–2100.

The climate projections were further refined using a modified version of the Reliability Ensemble Average (REA) methodology described by Giorgi & Mearns (2003). Herein, an averaging of the projections from the different GCMs was performed. The averaging was based on two criteria: model performance and model resemblance. For each criterion, the projections from the different GCMs were given a rank. Firstly, the models were ranked based on their ability to reproduce the historical climate in Bergen. This was achieved by comparing the monthly precipitation and mean monthly temperature produced by the GCMs over the reference period 1975–2005 with observations from the research site. Secondly, the monthly temperature for the period 2071–2100 and for each GCM were compared to the ensemble mean of each variable and RCP for the same period. The closer the GCM simulations were to the ensemble mean, the higher the rank. The ranks were given equal weights and combined into one overall reliability rank for each GCM.

Table 1 | List of selected GCMs for downscaling to 50540 Florida Weather Station

Model name	Modelling centre / group	Institute ID
bcc-csm1-1	Beijing Climate Center, China Meteorological Administration	BCC
CCSM4	National Center of Atmospheric Research	NCAR
CESM1-CAM5	Community of Earth System Model Contributors	NSF-DOE-NCAR
CSIRO-Mk3-6-0	Commonwealth Scientific and Industrial Research Organization in collaboration with Queensland Climate Change Centre of Excellence	CSIRO-QCCCE
FIO-ESM	The First Institute of Oceanography, SOA, China	FIO
GFDL-CM3	NOAA Geophysical Fluid Dynamics Laboratory	NOAA GFDL
GFDL-ESM2G	NOAA Geophysical Fluid Dynamics Laboratory	NOAA GFDL
GFDL-ESM2M	NOAA Geophysical Fluid Dynamics Laboratory	NOAA GFDL
GISS-E2-H	NASA Goddard Institute for Space Studies	NASA GISS
GISS-E2-R	NASA Goddard Institute for Space Studies	NASA GISS
HadGEM2-AO	Met Office Hadley Centre	MOHC
IPSL-CM5A-LR	Institute Pierre-Simon Laplace	IPSL
IPSL-CM5A-MR	Institute Pierre-Simon Laplace	IPSL
MIROC5	Atmosphere and Ocean Research Institute (The University of Tokyo), National Institute for Environmental Studies, and Japan Agency for Marine-Earth Science and Technology	MIROC
MIROC-ESM	Atmosphere and Ocean Research Institute (The University of Tokyo), National Institute for Environmental Studies, and Japan Agency for Marine-Earth Science and Technology	MIROC
MIROC-ESM-CHEM	Atmosphere and Ocean Research Institute (The University of Tokyo), National Institute for Environmental Studies, and Japan Agency for Marine-Earth Science and Technology	MIROC
MRI-CGCM3	Meteorological Research Institute	MRI
NorESM1-M	Norwegian Climate Centre	NCC
NorESM1-ME	Norwegian Climate Centre	NCC

Note: Overview and links to detailed model descriptions: http://cmip-pcmdi.llnl.gov/cmip5/availability.html.

Further, the reliability rank assigned to each GCM was used to calculate a weighted average of the temperature and precipitation projections, where a higher model rank gave the model higher weight in the averaging procedure. This was performed for three scenario intervals 2011–2040 (near term), 2041–2070 (medium term) and 2071–2100 (long term).

From this, change factors, i.e. the difference between historical climatology and downscaled climate projections, were calculated in accordance with the method outlined in Hamududu & Killingtveit (2016), where change factors for temperature are calculated as the absolute difference between observed and projected mean temperature and change factors for precipitation are calculated as the percentage difference between observed and projected precipitation. Change factors were calculated for each month of the year and for all scenario intervals.

Projections of future inflow

Inflow from the catchments surrounding the drinking water reservoirs in Bergen was projected using a hydrological model for the Bergen region (Kristvik & Riisnes 2015). The applied model is the lumped version of the conceptually based HBV model (Bergström 1976) for rainfall-runoff modelling. This model uses the change factors and historical records of daily temperature, precipitation and evapotranspiration as input to calculate the runoff in each catchment. In addition, the model takes in geographical parameters such as catchment area, hypsographic distribution, forest percentage, and lake percentage. The model structure consists of four storage elements: snow, soil moisture, upper zone, and lower zone. In each zone the inflow, storage level, and outflow to the next zone is calculated. Time series of daily temperature and precipitation to run the model were

collected from the main weather station in Bergen (station ID: 50540 Florida) while evapotranspiration was calculated based on temperature observations and projections using the Thornthwaite method. The existing HBV model distributes the monthly change factors over the inherent days of one month such that the model can run at a daily time step. Evidently, the delta change approach has a drawback in assuming stationarity of the daily distribution over the year and for only adding changes in amounts. However, given this paper's emphasis on water resource availability, daily variations are not needed. Simulations were run for the historical period 1980–2009 and the three scenario intervals (near, medium, and long term) for all RCPs.

Water availability index (WAI)

An index for water availability was defined to facilitate the analyses on the effects of different drivers on water availability in the future. Herein, water availability is defined as the total amount of water that is available for water supply when requirements to minimum storage reserves are accounted for. Minimum storage reserves (RR) refer to the volume of water that is always required in the reservoirs. The municipality in Bergen has set this threshold to a volume that corresponds to 50 days of consumption. The water availability index (WAI) is defined as the ratio between the available water and the capacity of the system to store water (Equation (1)):

$$WAI(t) = \frac{SW(t) - RR(t)}{SC} \tag{1}$$

where WAI(t) is the WAI at time t, SW(t) is the stored water at time t, RR(t) is the required storage reserves at time t, and SC is the installed storage capacity. Stored water, SW, is a reservoir balance considering all the water that enters the reservoirs and all that is withdrawn, such that:

$$WAI(t) = \frac{SW(t-1) + (Q_{in}(t) - Q_{out}(t))dT - RR(t)}{SC} \tag{2}$$

where Q_{in} represents the inflow from surrounding catchments to the drinking water reservoirs. As there are transfer tunnels in the distribution network of Bergen that

connect the treatment plants, the water balance is treated as a one-reservoir model where Q_{in} is the sum of all inflows to the various reservoirs. Q_{out} covers consumption, water lost to overflow when reservoirs are full, and a regulated flow of $12 \, m^3 \, s^{-1}$ that is released from the reservoir connected to the Espeland treatment plant during the period 1 April to 30 September. The consumption is defined as:

$$C_{tot} = (1 + a)C_{sp}P \tag{3}$$

where C_{tot} (m^3/timestep) is the total consumption, a is the leakage rate, C_{sp} (m^3/people/timestep) is the specific consumption related to the real consumption (e.g. domestic, industrial, and other), and P (people) is the total number of people supplied by the municipal water supply. C_{sp} was kept at a constant level of 241.3 liter/people/day (7.2 m^3/people/month) based on numbers provided by the municipality (Bergen Municipality 2015). The scenarios for population size, P, were based on population projections from Statistics Norway (2016b). Three scenarios from Statistics Norway's projections were selected: (1) the main alternative (MMMM); (2) low national growth (LLML); and (3) high national growth (HHMH). These scenarios provide projections until 2040 and were extrapolated until 2100 to match the length of the climate projections in this study. The extrapolated scenarios correspond to a monthly population growth of 177(MMMM), 88(LLML), and 301 (HHMH) people per month.

RESULTS AND DISCUSSION

The climatology for the reference period 1975–2005 simulated by the downscaled GCMs is presented in Figure 1 along with observed climatology for the same period. All GCMs are plotted, yielding a range of values for each month represented by the shaded areas. The bandwidth of this range varies for the two variables (temperature and precipitation) and for each month of the year. From visual inspection, it is observed that the offset is larger for precipitation amounts than average temperatures, i.e. the downscaling of temperature is more accurate. Furthermore, there is a general tendency of underestimation in

precipitation amounts in spring months (March, April, and May) overestimation in summer months (June, July, and August).

Mehran *et al.* (2014) investigated the bias between CMIP5 continental precipitation simulations and satellite-based gauge-adjusted observations, and found that, in general, monthly precipitation is well captured by most GCMs. However, inaccuracies of downscaled GCMs to the city of Bergen have been demonstrated. Due to their coarse spatial resolution, large-scale precipitation is not able to capture effects of local conditions, such as pronounced topography. Jonassen *et al.* (2013) demonstrated how spillover effects from certain mountains in Bergen strongly influence precipitation patterns, which could indicate limitations in using large-scale precipitation as predictor for local precipitation in Bergen. Nevertheless, the downscaled GCMs capture the seasonal variations over the year, characterized by high precipitation amounts in the colder months (winter and fall) and lower precipitation during spring and summer, which is considered adequate for the purpose of assessing long-term water availability.

Furthermore, variations in simulated climate can also be found in the future projections, as illustrated by Figure 2, which renders the distributions of the long-term change factors estimated from all downscaled GCMs and RCPs before

any weighting or averaging. The monthly projections span a wide range making the difference in projections across RCPs not easily detected visually. This span reflects the Type II uncertainty described by Ekström *et al.* (2015), discussed in the Introduction of this paper. Type II uncertainty comprises the uncertainty linked to the climate system's response to emissions. Using an ensemble of different GCMs, with different representations of the climate system and its processes, and gives a range of possible responses that capture this uncertainty. These results also illustrate the importance of using multi-model ensembles in climate impact studies, as the risk of a GCM being an outlier compared to the ensemble mean is high when using a single model.

The impacts of different emission scenarios are visualized in Figure 3, where the projections are reduced to change factors using the reliability ensemble averaging procedure. Temperature changes show a clear trend towards higher levels throughout the 21st century and increase in line with higher emission scenarios. Precipitation changes are less distinct, but also here, the highest emission scenarios result in the highest changes. The changes are in general positive (i.e. more precipitation) on an annual basis, however, they also imply increased variations between the dry spring and summer months and the rest of the year. The results are, to some degree, in agreement with other
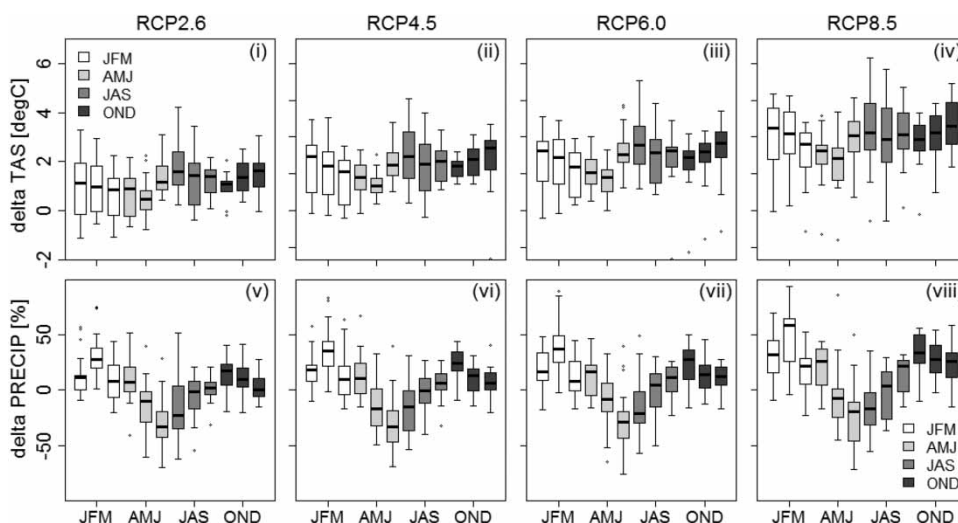

Figure 2 │ Long-term (2071–2100) monthly change factors for (i)–(iv) temperature and (v)–(viii) precipitation from the model ensemble. The figure shows the spread in change factors simulated by the GCMs, expressed by boxes restrained by the 75th (upper box limit) and 25th (lower box limit) percentiles. The simulation results are grouped by months of the year starting in January and ending in December.
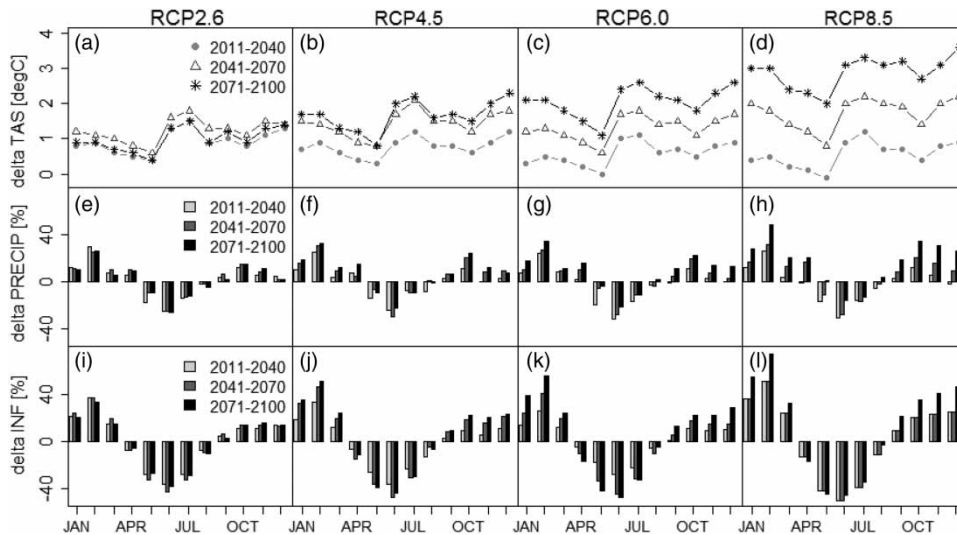
Figure 3 │ Computed change factors for (a)–(d) temperature, (e)–(h) precipitation and (i)–(l) total inflow from the reliability-based averaging procedure and hydrological simulations with the HBV model.

studies covering the region of Bergen. Projections for the county of Hordaland, in which the city of Bergen is located, are provided by Norwegian Centre for Climate Services (2016) (NCCS). In this report, the annual temperature is projected to increase by 4 °C and precipitation is expected to increase on an annual basis. The projections for spring and summer months differ, as NSSC project an increase in these months, rather than a decrease as suggested by the downscaling performed in this study. However, the downscaling made by NCCS is performed with a different methodology than the one outlined here, which might explain some of the divergent projections.

Figure 3 also depicts scenarios, represented as change factors, for future inflow to the drinking water reservoirs. The projected changes in inflow mirror the increased seasonal variations in precipitation amounts. They also reflect the impacts of rising temperatures. These are particularly evident in the month of April where a decrease in inflow is projected despite estimations of increasing precipitation. The decreasing inflows in April are likely to be a result of higher temperatures, less snow accumulation, and finally less snow melt during spring. The results are consistent with findings by Arnell (1999), who demonstrated that effects of climate change on hydrological extremes is likely to be strongest in regions where snow regimes are weakened due to higher temperatures, leading to heavier winter runoff

and decreased runoff during spring. Furthermore, due to higher temperatures and thus more evapotranspiration, the negative change factors in spring and summer are more severe for inflow than for precipitation.

Moreover, an increase of inflow during the remaining months of the year is projected. This increase indicates a potential for storage on both the near-, medium-, and long-term basis. To the projected scenarios, an increase of the storage capacity would allow for storing the increased inflow during winter such that the increased gap between dry and wet seasons is closed and a steady supply during summer months is secured.

The projected inflow scenarios are further used to calculate the WAI and the results are depicted in Figure 4. To assess the difference between the emission scenarios, all other variables (population growth, leakages, and storage capacity) are kept at a base level as rendered in Table 2. In this 'business-as-usual' scenario, leakages and storage capacity are kept at today's level, while the population projections follow the main alternative (MMMM) of Statistics Norway's population projections (Statistics Norway 2016b). The results show that the WAI is decreasing and the expected value is approximately the same for all emissions scenarios. However, the standard deviation increases with higher emissions scenario. The decreasing trend of the WAI implies a decrease in water supply security and
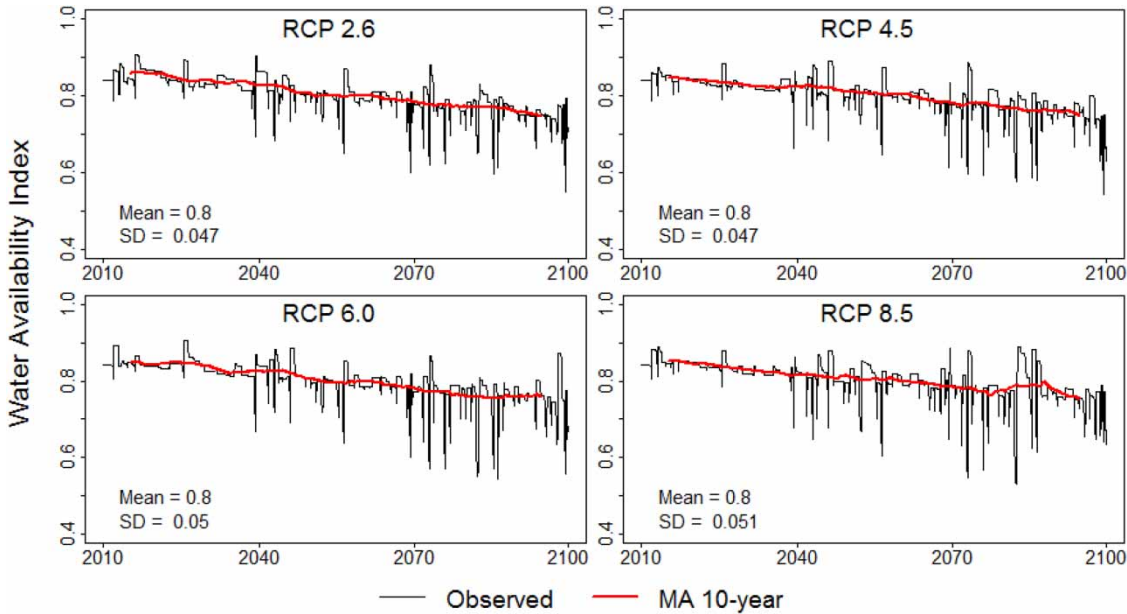
Figure 4 │ Computed WAI for varying inflow corresponding to the four emissions scenarios and base levels for leakages, population growth, and storage capacity. The time series are plotted with the moving average using a 10-year window.

increased vulnerability. Moreover, the increased standard deviation to the higher emissions scenarios indicates that the higher emissions lead to more unpredictable water availability.

Furthermore, the level of leakages, population growth and storage capacity were changed one by one (while the others were kept at base level) as given in Table 2.

Changing the parameters one by one afforded five additional scenarios: (1) low leakage rate (Leak L); (2) high leakage rate (Leak H); (3) low population growth (Pop L); (4) high population growth (Pop H); and (5) increased storage capacity (SC H). The results are presented in Figure 5. In all emission scenarios, the WAI is most sensitive to, and negatively affected by, population growth. There are two main reasons for this: increased population causes increased water consumption putting more strain

on stored water (SW); and the WAI is constrained by required storage reserves (RR), which are directly influenced by the population as the required volume equal to 50 days of consumption will increase with population growth. Moreover, the scenario for low population growth (Pop L) has the most positive impact on the WAI for each emission scenario. Furthermore, Figure 5 shows the effect of the counteractive measures (leakage reduction and increased storage capacity), as well as the effects of letting the leakage level exacerbate to higher levels (40%). Although it does not have as great an impact on the WAI as population growth, allowing leakages to reach a level of 40% will have a clear negative impact on the WAI. Reducing leakages to the desired level of 20% will have a positive impact. However, the effect of this level will have approximately the same effect on the WAI as increasing storage capacity by approximately 10% (illustrated by the coinciding plots of Leak L and SC H).

Demand management does not appear to be the only viable option for addressing low water availability in Bergen, as concluded by Xia *et al.* (2012) in their Chinese case study. On the contrary, several studies argue that increased storage capacity will help in coping with increased seasonal variations and that the necessity for dams will
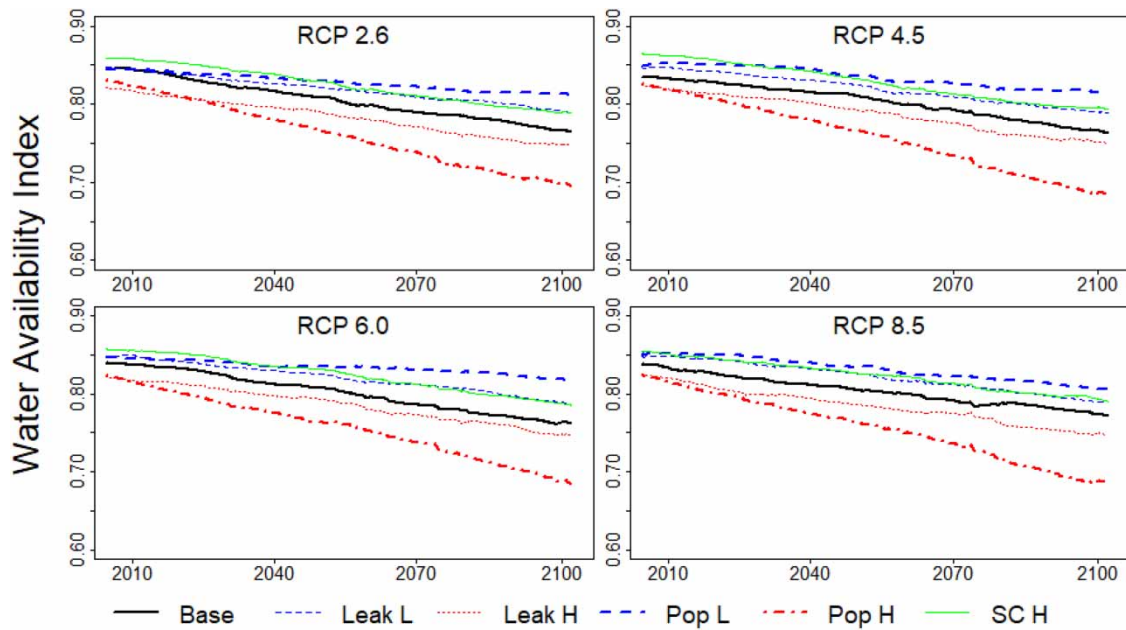
Table 2 │ Selected scenarios for sensitivity analysis of the WAI

Scenario	Leakages (%)	Population growth (people/month)	Storage capacity (Mm³)
Base	30	177	26.5
Low	20	88	26.5
High	40	301	30.0

Figure 5 | Sensitivity of computed WAI (10-year MA) to changes in leakages, population growth, and storage capacity.

increase (e.g. Ehsani *et al.* 2017), while others have found that a combined solution is more appropriate (Lopez *et al.* 2009). Ultimately, comparing the cost and benefit of supply vs. demand side measures could enrich the analysis and help determine the optimal action to be taken for the specific case of Bergen.

CONCLUSIONS

This paper has presented a framework for assessing future water availability in cities. The suggested framework is tailored to account for not only climatic changes at the local level, but also other factors that might put strain on future water supply, such as population growth and leakages in the distribution network. These driving forces are summarized in an index for water availability which has been demonstrated for use in scenario and sensitivity analyses.

Special focus has been given to downscaling of GCMs and refining climate scenarios at the local level. The downscaled GCMs offer a wide range of possible future climates in the city of Bergen, Norway. This spread in downscaled results highlights the need for further processing of the projections as demonstrated here by the reliability averaging

method. However, the large uncertainties linked to climate projections are still not fully excluded and need to be considered in further studies of water availability.

For this purpose, the WAI was introduced. This index allows for studying impacts on water availability under a range of various climate scenarios. Rather than predicting future water availability, this tool enables a climate-informed assessment. This flexibility makes it suitable for decision making under uncertainty. For transparency, other trends, such as population growth and deteriorating infrastructure are represented explicitly in the WAI. This makes the WAI a practical tool for water managers and decision makers in cities.

By applying the proposed framework, three main conclusions regarding future water availability in the city of Bergen, Norway, can be drawn. Firstly, the results of downscaling suggest higher seasonal variations in inflow and thus an increased potential for storage such that more water can be preserved for dryer seasons. Secondly, in a 'business-as-usual' scenario-analysis of the WAI indicated a more vulnerable water supply due to decreased and more unpredictable water availability. Finally, it was shown that the city's policy of reducing leakages to a level of 20% would have approximately the same effect on water availability as a 10%

increase in storage capacity. Along with socio-economic analyses of the costs of implementing such counteractive measures, this framework could form a solid basis for decision making.

REFERENCES

Arnell, N. W. 1999 The effect of climate change on hydrological regimes in Europe: a continental perspective. *Global Environmental Change* **9**, 5–23.

Barnett, T. P., Pierce, D. W., Hidalgo, H. G., Bonfils, C., Santer, B. D., Das, T., Bala, G., Wood, A. W., Nozawa, T., Mirin, A. A., Cayan, D. R. & Dettinger, M. D. 2008 Human-induced changes in the hydrology of the western United States. *Science* **319**, 1080–1083.

Benestad, R. E., Hanssen-Bauer, I. & Chen, D. 2008 *Empirical-statistical Downscaling*. World Scientific Publishing Company, London, UK and New Jersey, USA.

Benestad, R. E., Mezghani, A. & Parding, K. M. 2015 *ESD* V1.0. Zenodo, available at: http://dx.doi.org/10.5281/zenodo.29385.

Bergen Municipality 2015 Hovedplan for vannforsyning 2015-2024 (Strategic plan for water supply 2015-2024), Bergen. Available at: https://www.bergen.kommune.no/omkommunen/avdelinger/vannog-avlopsetaten/9081/article-129478 (Accessed online 6 October 2016).

Bergström, S. 1976 Development and application of a conceptual runoff model for Scandinavian catchments, Norrköping: SMHI RH07.

CMIP5 2013 Coupled Model Intercomparison Project Phase 5 – Overview. Available at: http://cmip-pcmdi.llnl.gov/cmip5/index.html?submenuheader=0 (Accessed March 23, 2017).

Ehsani, N., Vörösmarty, C. J., Fekete, B. M. & Stakhiv, E. Z. 2017 Reservoir operations under climate change: storage capacity options to mitigate risk. *Journal of Hydrology* **555**, 435–446.

Ekström, M., Grose, M. R. & Whetton, P. H. 2015 An appraisal of downscaling methods used in climate change research. *Wiley Interdisciplinary Reviews: Climate Change* **6**, 301–319.

Fowler, H. J., Blenkingsop, S. & Tebaldi, C. 2007 Linking climate change modelling to impacts studies: recent advances in downscaling techniques for hydrological modelling. *International Journal of Climatology* **27**, 1547–1578.

Giorgi, F. & Mearns, L. O. 2003 Probability of regional climate change based on the reliability ensemble averaging (REA) method. *Geophysical Research Letters* **30**, 2–5.

Hamududu, B. H. & Killingtveit, Å. 2016 Hydropower production in future climate scenarios; the case for the Zambezi River. *Energies* **9**, 1–18.

IPCC 2013 *Climate Change 2013: The Physical Science Basis. Contribution of Working Group I to the Fifth Assessment Report of the Intergovernmental Panel on Climate Change*, Cambridge University Press, Cambridge, United Kingdom and New York, NY, USA.

Jonassen, M. O., Ólafsson, H., Valved, A. S., Reuder, J. & Olseth, J. A. 2013 Simulations of the Bergen orographic wind shelter, *Tellus A* **65** (1), 1–17. doi:10.3402/tellusa.v65i0.19206.

Kalnay, E., Kanamitsu, M., Kistler, R., Collins, W., Deaven, D., Gandin, L., Iredell, M., Saha, S., White, G., Woollen, J. & Zhu, Y. 1996 The NCEP/NCAR 40-year reanalysis project. *Bulletin of the American Meteorological Society* **77**, 437–471.

Kristvik, E. & Riisnes, B. 2015 *Hydrological Assessment of Water Resources in Bergen*. MS thesis, Norwegian University of Science and Technology, Trøndheim, Norway.

Lopez, A., Fung, F., New, M., Watts, G., Weston, A. & Wilby, R. L. 2009 From climate model ensembles to climate change impacts and adaptation: a case study of water resource management in the southwest of England. *Water Resources Research* **45**, W08419. doi: 10.1029/2008WR007499.

Maraun, D., Wetterhall, F., Chandler, R. E., Kendon, E. J., Widmann, M., Brienen, S., Rust, H. W., Sauter, T., Themeßl, M., Venema, V. K. C., Chun, K. P., Goodess, C. M., Jones, R. G., Onof, C., Vrac, M. & Thiele-Eich, I. 2010 Precipitation downscaling under climate change: recent developments to bridge the gap between dynamical models and the end user. *Reviews of Geophysics* **48** (2009RG000314), 1–38.

Mehran, A., Aghakouchak, A. & Phillips, T. J. 2014 Evaluation of CMIP5 continental precipitation simulations relative to satellite-based gauge-adjusted observations. *Journal of Geophysical Research* **119**, 1695–1707. http://doi.wiley.com/10.1002/2013JD021152 (Accessed March 15, 2017).

Moss, R. H., Edmonds, J. A., Hibbard, K. A., Manning, M. R., Rose, S. K., Van Vuuren, D. P., Carter, T. R., Emori, S., Kainuma, M., Kram, T., Meehl, G. A., Mitchell, J. F. B., Nakicenovic, N., Riahi, K., Smith, S. J., Stouffer, R. J., Thomson, A. M., Weyant, J. P. & Wilbanks, T. J. 2010 The next generation of scenarios for climate change research and assessment. *Nature* **463**, 747–756.

Norwegian Centre for Climate Services 2016 Klimaprofil Hordaland (Climate profile for Hordaland county), available at: https://klimaservicesenter.no/faces/desktop/article.xhtml?uri=klimaservicesenteret/klimaprofiler/klimaprofil-hordaland (Accessed online 5 December 2016).

Plummer, R., de Loë, R. & Armitage, D. 2012 A systematic review of water vulnerability assessment tools. *Water Resources Management* **26**, 4327–4346.

Schewe, J., Heinke, J., Gerten, D., Haddeland, I., Arnell, N. W., Clark, D. B., Dankers, R., Eisner, S., Fekete, B. M., Colón-González, F. J. & Gosling, S. N. 2014 Multimodel assessment of water scarcity under climate change. *Proceedings of the National Academy of Sciences* **111**, 3245–3250.

Statistics Norway 2016a Municipal water supply, Table 04689: I. Water – basic data (M). Available at: https://www.ssb.no/en/natur-og-miljo/statistikker/vann_kostra (Accessed November 7, 2016).

Statistics Norway 2016b Population projections, Table 11168: Population projections 1 January, by sex and age, in 9 variants (m). Available at: https://www.ssb.no/en/befolkning/statistikker/folkfram (Accessed December 3, 2016).

Sullivan, C. A. 2011 Quantifying water vulnerability: a multi-dimensional approach. *Stochastic Environmental Research and Risk Assessment* **25**, 627–640.

Tønnessen, M. & Leknes, S. 2016 Population projections 2016–2100: Main results. Available at: http://ssb.no/en/befolkning/artikler-og-publikasjoner/population-projections-2016–2100-main-results (Accessed online 22 November 2016).

Whateley, S., Steinschneider, S. & Brown, C. 2014 A climate change range-based method for estimating robustness for water resources supply. *Water Resources Research* **50**, 8944–8961.

Wilby, R. L., Dawson, C. W. & Barrow, E. M. 2002 SDSM – a decision support tool for the assessment of regional climate change impacts. *Environmental Modelling & Software* **17**, 145–157.

Xia, J., Qiu, B. & Li, Y. 2012 Water resources vulnerability and adaptive management in the Huang, Huai and Hai river basins of China. *Water International* **37**, 523–536.